FES Control of Isometric Forces in the Rat Hindlimb Using Many Muscles

Anthony M. Jarc, Max Berniker, and Matthew C. Tresch

***Abstract*—Functional electrical stimulation (FES) attempts to restore motor behaviors to paralyzed limbs by electrically stimulating nerves and/or muscles. This restoration of behavior requires specifying commands to a large number of muscles, each making an independent contribution to the ongoing behavior. Efforts to develop FES systems in humans have generally been limited to pre-programmed, fixed muscle activation patterns. The development and evaluation of more sophisticated FES control strategies is difficult to accomplish in humans, mainly because of the limited access of patients for FES experiments. Here, we developed an in vivo FES test platform using a rat model that is capable of using many muscles for control and that can therefore be used to evaluate potential strategies for developing flexible FES control strategies. We first validated this FES test platform by showing consistent force responses to repeated stimulation, monotonically increasing muscle recruitment with constant force directions, and linear summation of co-stimulated muscles. These results demonstrate that we are able to differentially control the activation of many muscles, despite the small size of the rat hindlimb. We then demonstrate the utility of this platform to test potential FES control strategies, using it to test our ability to effectively produce open loop control of isometric forces. We show that we are able to use this preparation to produce a range of endpoint forces flexibly and with good accuracy. We suggest that this platform will aid in FES controller design, development, and evaluation, thus accelerating the development of effective FES applications for the restoration of movement in paralyzed patients.**

***Index Terms*—functional electrical stimulation, isometric force, muscle stimulation, rat hindlimb.**

I. Introduction

Functional electrical stimulation (FES) attempts to restore motor behaviors to paralyzed limbs by electrically stimulating nerves and muscles [1-3]. The long-term goal of FES research is to return patients to their functional state before the injury. In order to achieve this goal, FES systems must be able to flexibly coordinate the activation of a large number of muscles throughout the paralyzed limb. FES studies in humans have stimulated a large of number of muscles to restore behaviors such as standing [4, 5], walking [5-7], or grasping [8-12]. However, these FES systems typically restore a single motor act (or a few similar behaviors) by modulating a fixed pattern of activations. For example, in the Freehand system [13], muscles are activated in a fixed pattern in order to restore hand grasp. Although this activation helps restore functional ability to patients, the limited number of activation patterns restricts the motor repertoire available to the patient. To restore a broad range of motor behaviors it is necessary that stimulation patterns can be flexibly adjusted according to varying task demands.

Because it is difficult to develop novel FES controllers in human patients due to their limited accessibility, investigators have used animal models to develop and evaluate FES controllers. Animal models for FES have demonstrated control of basic motor functions including reaching [14, 15], grasping [14, 16, 17], and stepping [18-20]. These animal models, however, are often limited to activation of only a few muscles acting on the major degrees of freedom at individual joints. As a result these FES systems might not have the flexibility required to restore a wide range of movements and to adapt to the different environments or external conditions commonly encountered in daily living [21]. For example, in addition to flexor/extensor muscles about the hip or ankle, abductors and adductors at these joints might be required to maintain the proper stance phase and forward momentum of the body's center of mass during locomotion on uneven terrain [22, 23]. Additionally, these studies might inadvertently neglect the advantages of coordinating many muscles (e.g. regulation of additional properties such as joint stiffness) [23] or methods to deal with muscle redundancy. These are important design considerations for any FES controller whose ultimate performance must be evaluated in terms of restored behaviors in human patients.

In this study, we developed a FES test platform using the rat hindlimb that allows for the design and evaluation of complex FES control strategies. This work builds on previous studies using the rat as a model for FES [24-26] by substantially increasing the number of controlled muscles, developing methods for reliable measurements of evoked forces, and systematically testing basic assumptions of FES control (e.g. linear summation of forces and minimal current spillover). We describe the details of our test platform and demonstrate its utility for the development and evaluation of FES

Manuscript received August 5, 2012. We would like to acknowledge our funding sources for this research: NIH F31NS068030-01 (AMJ), NIH 1R01NS063399 (MB), and NIH R21NS061208 (MCT).

A. M. Jarc was with Northwestern University, Chicago, IL 60611 USA. He is now with Intuitive Surgical, Inc., Sunnyvale, CA 94086 USA (phone: 224-688-2307; e-mail: anthony.jarc@gmail.com).

M. Berniker is with Northwestern University, Chicago, IL 60611 USA (e-mail: m-berniker@northwestern.edu).

M.C. Tresch is with Northwestern University, Chicago, IL 60611 USA (e-mail: m-tresch@ northwestern.edu).

controllers by designing a controller capable of achieving a wide range of isometric force tasks using many muscles. We demonstrate that this controller performed well in producing a range of force directions and amplitudes. These results demonstrate the utility of our platform for the development of novel FES control strategies that can restore flexible motor behaviors to paralyzed patients.

II. Methods

A. Surgical procedure

All procedures were conducted under protocols approved by Northwestern University's Animal Care and Use Committee. The surgical procedure was modified from Yeo et al. [24]. Eight female, adult Sprague Dawley rats (250-300g) were initially anesthetized using 80mg/kg ketamine and 10mg/kg xylazine. The level of anesthesia was monitored throughout the experiment by toe pinch and maintained using intraperitoneal injection of 40mg/kg ketamine and 5mg/kg xylazine, as needed. Temperature was monitored using a rectal thermometer and core temperature was maintained between 36-38°C using a heating lamp. Heart rate and respiration were visually monitored to further ensure the viability of the animal throughout the experiment. One milliliter of saline was given every two hours to prevent dehydration.

Pelvic posts were implanted in the rostral and caudal contralateral pelvis and the rostral ipsilateral pelvis to isolate movement (Fig. 1A). The site of the pelvis implant was initially identified through manual palpation. An incision was then made through the gluteal muscles (rostral) and the hamstrings muscles (caudal) to expose the pelvis. A 1.25mm pilot hole was drilled perpendicular to the surface of the pelvis. Then, 1.5mm diameter, 3cm long self-tapping bone pins (IMEX Veterinary, Inc.) were screwed directly into the pelvis to provide maximal stability. Bone cement (Durelon, 3M) was placed on the threads of the bone pins as they were inserted and then on the surface of the bone around the bone pins once inserted to provide additional fixation. During initial development, the pelvic fixation included only contralateral posts. This provided enough stability to eliminate any visible skeletal movement during the production of usual isometric forces. When larger forces were evoked, however, either from individual muscles or from a combination of muscles, we often saw movement of the skeleton due to the internal flexibility of the pelvis. An ipsilateral pelvic post was necessary to reduce this internal motion sufficiently so as to accurately characterize muscle actions. However, because implantation of this post required dissection of gluteal muscles, we were unable to implant and stimulate these muscles.

A threaded rod (0.27cm diameter) was affixed to the distal tibia near the ankle to interface with a force transducer. After an incision was made to expose the medial surface of the tibia, two #00 screws (J.I. Morris Company) were screwed into the bone, spaced approximately 0.5cm apart. Bone cement was then used to secure the threaded rod to the screws. Finally, the rod was screwed into the free end of a six-axis force transducer (ATI Industrial Automation) to measure isometric endpoint forces and moments (Fig. 1A and 1B).

Experiments were conducted until the health of the animal degraded to a point where inconsistent breathing and a drop in core temperature were observed. Once this occurred, typically after about 6 hours, the animal was euthanized using a 1ml intraperitoneal injection of Euthasol followed by a bilateral thoracotomy. Post-mortem dissections were performed to ensure proper placement of intramuscular electrodes in the targeted muscles as well as to examine the integrity of the electrodes (e.g. dislodgement or breakage) for those muscles whose measured forces were no longer present or changed significantly during the course of the experiment.

B. Electrode design and implantation

Monopolar stimulating electrodes were constructed using seven-stranded, Teflon insulated steel wire (0.055in diameter, A-M Systems, Inc.). A knot was made at one end and a wax bead placed over the knot to prevent the electrode from slipping through the muscle once inserted and to insulate the cut end of the electrode (Fig. 1C). Approximately 0.0-0.5cm from the wax bead, insulation was removed from the wire to serve as a stimulation site. The amount of insulation removed from the electrode (0.1-0.5cm) along with the exposure's distance from the wax bead was customized for each muscle to optimize stimulation of the muscle's motor point. The opposite end of the wire was de-insulated and attached to the stimulator (FNS-16 Multi-Channel Stimulator, CWE, Inc.) via a break-out board.

A medial incision on the hindlimb was made to expose the medial muscles and an incision directly over the femur was made to expose the lateral hindlimb muscles. The motor points of the muscles were determined by using a handheld probe (continuous biphasic stimulation at 1Hz, 1mA pulse amplitude, 0.1msec pulsewidth) to visually identify the location within each muscle where the most complete muscle contraction occurred. With this technique up to 11 muscles were implanted with the monopolar stimulating electrodes.

Two common returns for all stimulating electrodes were also implanted. The returns were custom-sized brass plates (1cm by 2cm and 0.5mm thick) with a connecting wire soldered to the end of the plate that traveled transcutaneously to the stimulator. The common returns were placed along the lateral side of the animal rostral to the hindlimb and directly over the belly of the animal medial to the hindlimb. This minimized the unintentional activation of other muscles during stimulation, a phenomenon commonly referred to as current spillover. We evaluated traditional common return designs [25, 27] before choosing the final design that used a large surface area (via the two plates) to decrease charge density and therefore reduce current spillover during stimulation.

Most of the targeted muscles were chosen because of their relatively large size and ease of access for surgical implantation. Since the foot was not attached to the force transducer, distal muscles spanning the ankle were not used as they would have produced ankle movements and consequent reaction torques at the force transducer. The muscles used for

stimulation included biceps femoris anterior (BFa) and posterior (BFp), semitendinosus (ST), semimembranosus (SM), adductor magnus (AM) and longus (AL; activated together), vastus medialis (VM), vastus lateralis (VL), rectus femoris (RF), iliopsoas (IP), gracilius anticus (GRa) and posticus (GRp; activated together), and caudofemoralis (CF).

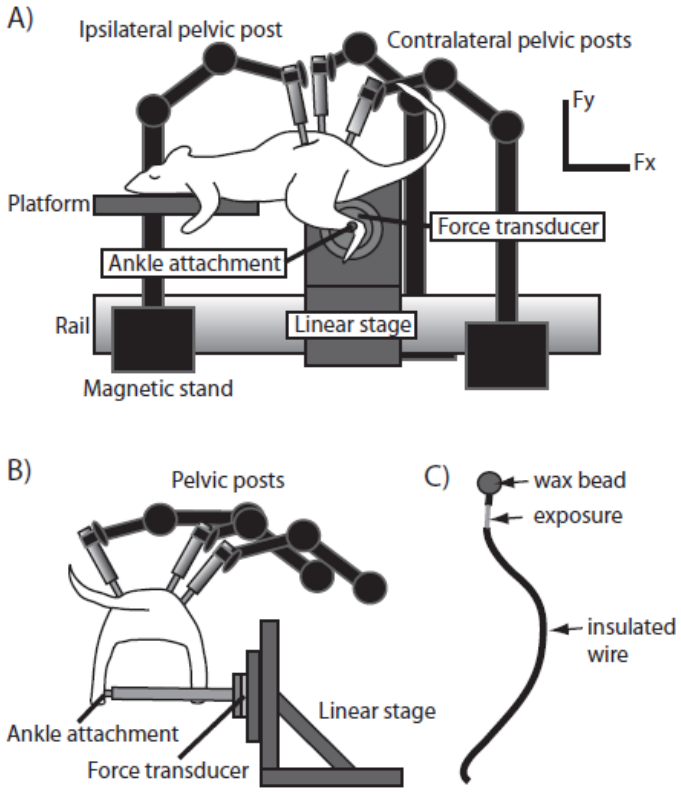

Fig. 1. Schematic of FES test platform. A) Illustration of pelvic fixation and ankle attachment to a force transducer. B) Rear view of test platform. C) Stimulation electrode design with an exposure that is situated near the motor point of targeted hindlimb muscles.

C. Isometric endpoint force measurement

The three pelvic posts were secured using flexible arms atop magnetic stands to prevent movement of the pelvis. The threaded ankle attachment was connected to a six-axis force transducer (ATI Mini 40) on the medial side of the hindlimb. The posture of the hindlimb was adjusted to be well within the joint ranges of motion, with the foot below the hip and the knee flexed approximately 90°. Once the animal was secured in the test platform, intramuscular stimulation evoked endpoint forces with minimal movement of the pelvis or internal movement of hip and knee joints. Endpoint forces were evoked by stimulating individual muscles with a biphasic current train. A stimulation frequency of 75Hz was used since it produced fused tetanus and was consistent with previous studies [25]. The pulsewidth of the stimulation trains remained fixed at 0.1msec whereas the pulse amplitude typically varied between 0.05mA and 4mA depending on the muscle and the desired force vector. The stimulation trains were delivered for 0.5 seconds. Though our stimulation trains lasted only 0.5 seconds, the resulting force responses consistently achieved steady-state plateaus, likely because of our good skeletal fixation.

D. Co-stimulated muscle forces

The linear summation of isometric forces produced during muscle co-stimulation is a crucial assumption within most FES applications. If this assumption were not valid, then predicting the consequences of combined muscle activations would be very difficult. We tested this assumption for our preparation by first stimulating each muscle independently and, after waiting 90 seconds to prevent fatigue, stimulating the two muscles together. We completed 26 muscle co-stimulation trials across four experiments. The pairs of co-stimulated muscles were chosen randomly from the possible eleven muscles. We quantified the linearity of the combined stimulation by computing the coefficient of determination (R^2) with respect to the unity line (indicating perfect linearity) for the relationship between predicted and actual co-stimulation forces. The x and y force components were evaluated separately.

E. Recruitment curves

For each muscle, recruitment data was generated by modulating the pulse amplitude of biphasic, 0.5 second stimulation trains (0.1msec pulsewidth, 75Hz stimulation frequency) and measuring the evoked force. Ten stimulation trials were collected for each muscle across a range of pulse amplitudes. The range of pulse amplitudes used for each muscle was determined from initial experiments so that the entire range of force magnitudes (from threshold to plateau) was evoked. The steady-state period (the final 250msec of the 0.5 second stimulation trains) of the force magnitude was used as the resultant force. Recruitment curves were created by fitting sigmoids to the recruitment data using least-squares. The sigmoid function is shown in (1), where u is stimulation strength and α, β, γ, and δ are free parameters.

$$f(u) = \alpha + \beta\left(\frac{1}{1+e^{\gamma(u-\delta)}}\right) \quad (1)$$

We quantified the ability of sigmoid functions to capture the recruitment properties of muscles by computing the mean squared residual of the sigmoidal fit compared to the data.

F. Open loop FES control

Five animals were used to demonstrate feedforward FES control of isometric forces. For each animal, up to eleven muscles were successfully implanted with intramuscular stimulating electrodes. Recruitment curves were collected for each muscle and used to produce randomly chosen isometric forces. A total of 241 control trials were performed.

Using the recruitment curves of up to eleven muscles, an optimization routine was used to define stimulation parameters for arbitrary two-dimensional force vectors throughout the feasible force space of the hindlimb [28]. The optimization minimized a cost function that balanced accuracy (i.e. achieving the desired force) and effort (i.e. minimizing the squared total activation across all muscles used) while

constraining activations to be positive ($x > 0$), as shown in (2).

$$c = x^T Rx + \left(F_{hat} - F_{des}\right)^T Q\left(F_{hat} - F_{des}\right) \qquad (2)$$

Initially, we started with equal weights for efficiency, R, and accuracy, Q. The efficiency weight was then adjusted to a value at which the desired force vector was predicted and any further increase caused an error in the predicted force vector.

The muscles of the rat hindlimb were then stimulated according to the optimal stimulation patterns. The resulting force vectors were compared to the desired force vectors. Between 5 and 10 desired force targets were chosen during each set of control trials. The targets were randomly selected for stimulation. Depending on the health of the animal, between 1-10 sets of control trials were collected for each animal with recruitment curves directly preceding each set.

G. Error Analysis

The accuracy of the force control was quantified by comparing the observed force vector to the desired force vector. The two vectors were compared by measuring the Cartesian distance between the force vectors. In addition, the vectors were compared by calculating a normalized error, $\tilde{e}$, according to (3), where F_{actual} is the actual force produced and F_{des} is the desired force.

$$\tilde{e} = \left\|F_{actual} - F_{des}\right\| / \left\|F_{des}\right\| \times 100 \qquad (3)$$

Note that although this normalized error is useful since it can be interpreted as a percent error and standardizes the error across force vector magnitudes, the normalization magnifies the uncertainty in forces due to measurement noise for small vectors (see Fig. 8). We also evaluated the accuracy of control by examining the relationship between the individual components of the desired forces (e.g. F_x and F*y*) and the actual force components. If perfect control were observed, the forces would fall on the identity line. Finally, we examined the pattern of error across the workspace of the limb for all experiments using a contour plot. A cubic spline interpolation was used to estimate the raw errors across the range of forces that was examined. This contour plot was found using data combined across all animals.

III. Results

A. Force production from stimulation of individual muscles

An example of the forces produced from several stimulation trials in an implanted muscle (BFp) is shown in Fig. 2A. In each trial, the evoked force magnitude increased smoothly, reaching a plateau approximately 50 milliseconds following stimulation onset. Fig. 2B shows that as stimulation strength was increased the evoked force magnitude increased monotonically with minimal change in the direction of the evoked force. These results are summarized in Fig. 2C and 2D, showing the relationship of evoked force magnitude and force direction (measured at steady state as indicated in Fig. 2A) to the stimulation strength. As shown for the example illustrated in the figure, force magnitude reached a maximum around 1mA and increased only minimally at higher stimulation strengths. The direction of the evoked force varied less than 3 degrees in the sagittal plane across different stimulation strengths. The absence of abrupt changes in the evoked forces (in either magnitude or direction) suggests that these stimulations evoked isolated activation of this muscle. The absence of directional changes also indicates that there was minimal movement of the skeleton during these evoked responses, even for the relatively large magnitude responses of biceps femoris posterior shown in Fig. 2. Most muscles used in this study behaved similarly to the example illustrated in Fig. 2.

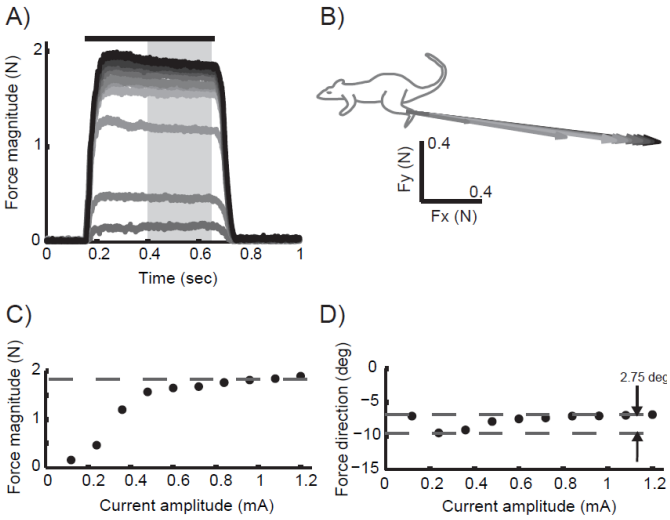

Fig. 2. Isometric force responses from biceps femoris posterior using our FES test platform. A) Raw force magnitude traces achieve fused tetanus and steady-state values for multiple stimulation strengths. The constant stimulation train is indicated by the black line above the force traces. The gray section indicates the range of forces used to find the average force response for a given stimulation. B) The resultant force responses (shown in the Fx-Fy space) maintained a consistent direction with increasing stimulation strength. Inset coordinate frame indicates force direction and associated angle, β. C) The force magnitude monotonically increased with stimulation strength. D) The force direction was constant across stimulation strength. Rat schematic modified from Tresch and Bizzi [29].

B. Linearity of muscle co-stimulation

The above results demonstrate our ability to activate individual muscles in the rat hindlimb independently and predictably. In order to be useful for FES applications, however, it is necessary that activation of multiple muscles also produces predictable responses. In particular, the forces evoked from stimulation of individual muscles should add linearly. Current spillover to adjacent muscles, internal motion of the skeleton, nonspecific muscle activation due to the return electrode, as well as connective tissue interactions between muscles [30, 31] all might be expected to lead to nonlinear interactions between evoked forces. If this were the case, then building FES controllers would be substantially complicated, requiring the characterization of the high-dimensional,

nonlinear interactions between muscle stimulation patterns and evoked forces.

We therefore evaluated the linearity of combined muscle stimulation by comparing the force response observed from simultaneous stimulation of two muscles to the force response predicted from the linear combination of the force responses evoked from each muscle separately. Three examples of this type of co-stimulation are shown in Fig. 3A-C. As can be seen in the figure, whether the muscles were partial synergists, synergists, or antagonists (as defined by the direction of the evoked force) their responses added approximately linearly. As shown in Fig. 3D and E, this linearity was observed across the 23 trials we performed, in that the slope between the observed and predicted forces was close to unity (for x component of the force $R^2_x = 0.91$, for the y component of the force $R^2_y = 0.93$).

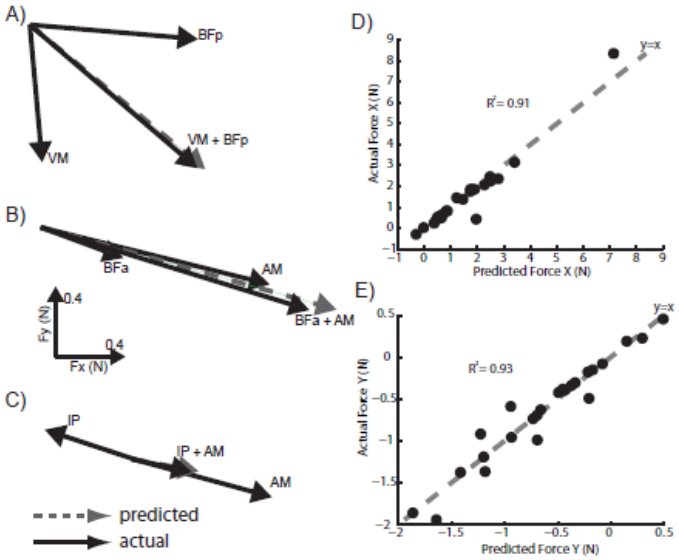

Fig. 3. Example force vectors from muscle co-stimulations and comparisons of actual and predicted isometric forces during muscle co-stimulation trials. In A-C, black vectors correspond to individual muscle force responses and the actual co-stimulation of two muscles. The predicted linear summation of the two independent muscle forces is represented as a grey, dashed vector. A) Partial agonists, VM and BFp. B) Complete agonists, BFa and AM. C) Antagonists, IP and AM. In D and E, R^2 values represent a measure of accuracy. D) Force in the x-direction. E) Force in the y-direction. The black dots in D and E correspond to trials across four experiments.

C. Recruitment curve characterization

The first step of open loop FES control in this study was to identify muscle recruitment properties. Similar to other studies [32-34], we assumed a sigmoidal relationship between force magnitude and stimulation strength. Force direction was assumed to be constant across stimulation strength. This assumption of constant direction was well supported by the observed responses, with the average change in direction being 3.84 +/- 11.96 degrees (see Fig. 2). An example of the recruitment curves measured for all muscles in one animal is shown in Fig. 4. As can be seen in the figure, there was a range of shapes of recruitment curves across muscles. While the recruitment curves of some muscles were steep (e.g. SM, RF, and BFa), others were relatively shallow (e.g. AM, IP, VM). For each muscle, however, the recruitment curve was well described as a sigmoid, as can be seen by the close relationship between the data points and the sigmoidal fit. The fraction of variance explained by the fit for this animal was very high, being greater than 0.99 for each muscle. These results were similar across animals, with the average R^2 value being 0.89 +/-0.25 for all muscles and all animals.

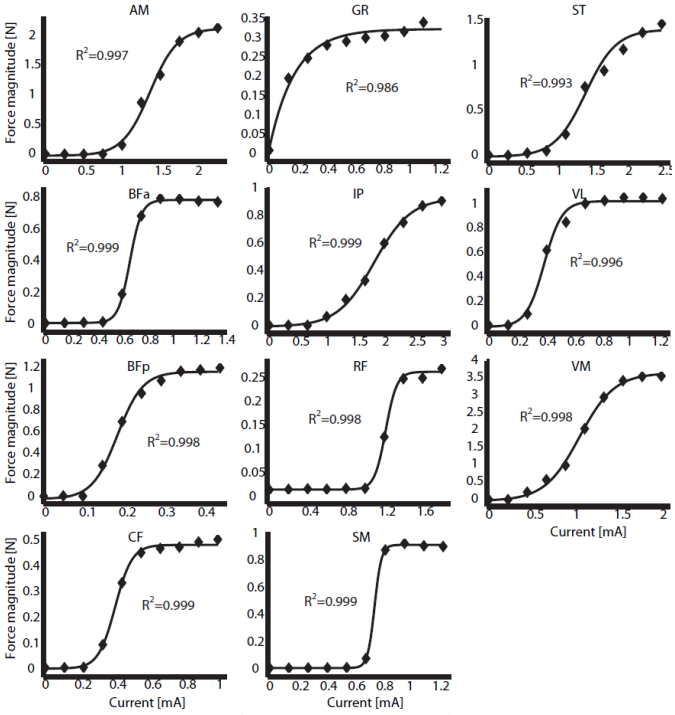

Fig. 4. Recruitment curves for the 11 muscles used for control. The individual points (black diamonds) correspond to the average steady-state force at the given current or stimulation strength. The sigmoid curves were fit to this force data and R^2 values quantified the goodness of fit.

D. Isometric force control

We then performed open loop FES control of isometric force vectors, using the sigmoidal recruitment curves described in the previous section. Examples of open loop FES control of isometric forces in the sagittal plane are shown in Fig. 5 for one animal. As shown in the figure, the observed forces (black, solid vectors) are very similar to the desired forces (grey, dashed vectors) across a broad range of force directions and magnitudes. Note also the consistency of the observed forces across repeated stimulation trials. Fig. 6 shows the relationship between observed forces and desired forces for all trials and all animals. In general, the relationship between observed and desired forces was close to unity, for both the x-component ($R^2 = 0.89$) and the y-component of the force ($R^2 = 0.90$). The accuracy of the control was roughly similar across all animals (Table 3). The average raw error across all experiments was 0.37N (+/- 0.018N). The normalized error across all trials was 27.49% (+/-1.35%). The average absolute direction error (in the sagittal plane) was 8.96 degrees (+/-0.92 degrees) while the absolute, normalized magnitude error was 21.07% (+/-1.49%) or 0.27N (+/- 0.012N). Taken together, these results indicate that we were able to consistently produce desired forces with good accuracy

across the range of forces.

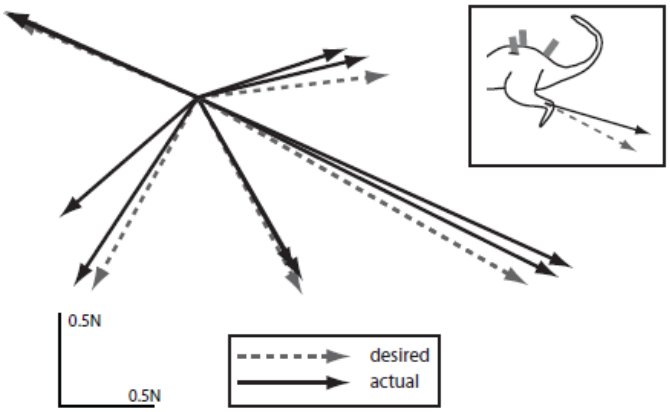

Fig. 5. Example force trials (black, solid vectors) of open loop FES control to desired force vectors (grey, dashed vectors) in the sagittal plane. Two repetitions to each desired force were performed non-sequentially. Refer to the inset for the relation between the forces and the rat hindlimb. Rat schematic modified from Tresch and Bizzi [29].

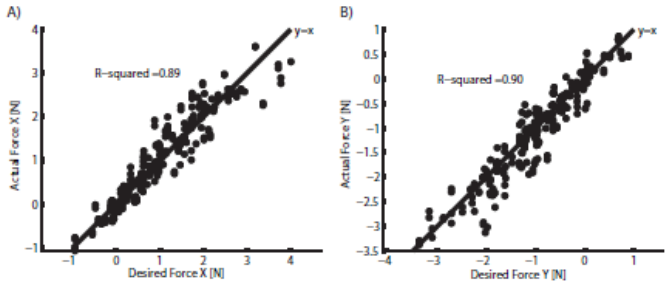

Fig. 6. Correlations between actual and desired force components. A) Forces in the x-direction. B) Forces in the y-direction. Data combined from five different experiments. Reported R^2 is across all experiments.

We next examined whether the magnitude of the error was systematically related to features of the stimulation trials. Fig. 7 shows how the error varied across the range of desired forces examined in these experiments. As seen in the plot there was a tendency for the error to be larger for larger desired forces. This tendency was more apparent for desired forces directed in extension, for which it was possible to evoke larger force vectors. In Fig. 8A, we illustrate the relationship between error magnitude and desired force magnitude, showing that there was a small positive correlation ($p<0.001$) consistent with the results of Fig. 7.

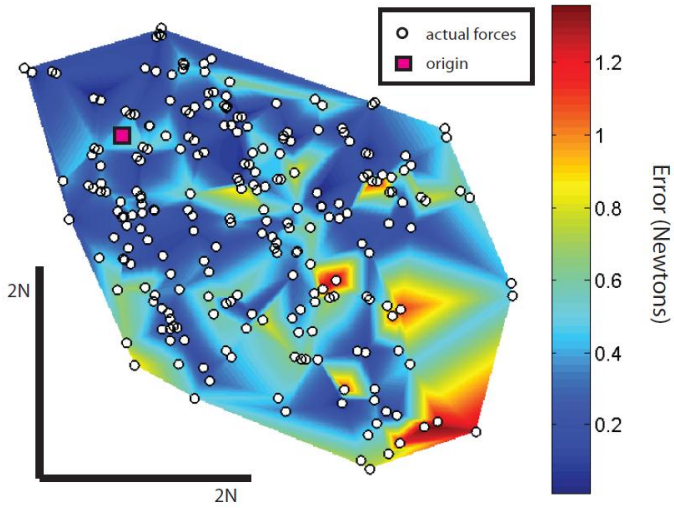

Fig. 7. Contour plot of the raw error during feedforward FES control of isometric forces. The error in regions unoccupied by actual forces (white circles) was interpolated.

Note that the analyses in Fig. 7 and 8 were performed using the raw, un-normalized error rather than the commonly used normalized error (3). Although this measure is commonly used, we found that it could result in misleading conclusions. For instance, we found an apparent negative correlation between the normalized error magnitude and the magnitude of the desired force (Fig. 8B), in contrast to the positive correlation found using the un-normalized error (Fig. 7). This negative correlation using the normalized error reflects the amplification of errors for small vectors by the normalization process. In fact, if we assume a constant error (estimated as 0.37N, as described above) across all desired force magnitudes and then calculated the normalized error, we obtained the curved line shown in Fig. 8B which captured the observed negative correlation between normalized error and force magnitude in the observed data set. This result shows that the normalized error, although commonly used to quantify controller performance, distorts errors for small vectors.

Since the overall error involves both force magnitude and force direction, we also examined how these two properties varied with force magnitude (Fig. 8C and 8D, respectively). Indeed, the same general relationship existed as normalized error where smaller desired forces, on average, had larger magnitude and direction errors.

TABLE I
ERROR METRICS ACROSS ALL EXPERIMENTS

Exp.	Norm. Error (+/- SE) [%]	Raw Error (+/- SE) [N]	|Dir. Error| (+/- SE) [deg]	|Mag. Error| (+/- SE) [%]
1	28.43 (2.76)	0.54 (0.067)	9.38 (1.04)	20.88 (2.74)
2	34.29 (3.47)	0.39 (0.026)	10.88 (2.95)	28.10 (2.96)
3	20.92 (2.72)	0.35 (0.034)	4.93 (0.77)	17.90 (2.58)
4	23.79 (3.11)	0.24 (0.025)	8.35 (1.61)	15.80 (1.95)
5	30.04 (5.95)	0.32 (0.048)	11.25 (2.44)	22.68 (5.81)
All	27.49 (1.35)	0.37 (0.018)	8.96 (0.92)	21.07 (1.49)

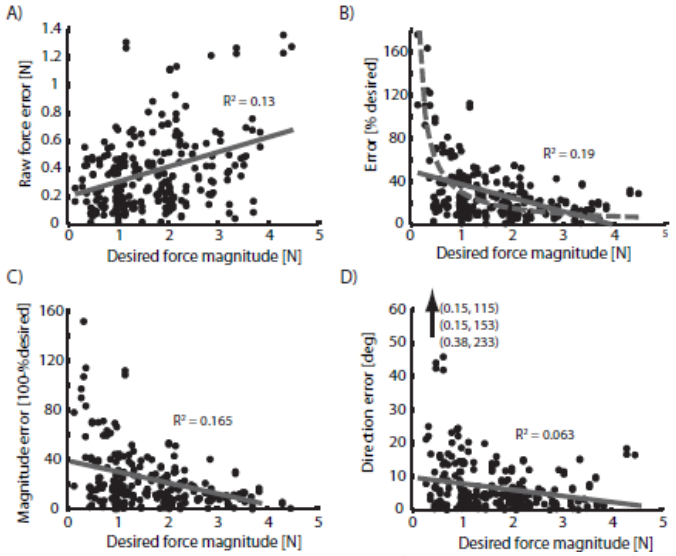

Fig. 8. Error metrics with respect to desired force magnitude. A) Raw force error. B) Normalized error. C) Magnitude error. D) Direction error. Each point corresponds to a single force trial. Five different experiments are represented. Linear fits and their corresponding R^2 values were reported. An inverse relationship between normalized error and force magnitude was also shown in B) as a grey, dashed line.

IV. Discussion

In this study, we developed and validated a FES test platform using the rat hindlimb, showing that we were able to stimulate individual muscles independently and reliably. We also demonstrated accurate open loop FES control of isometric forces using many muscles. Our results establish that this preparation can be used for *in vivo* evaluation of FES control strategies that attempt to restore functional behaviors prior to their application in human subjects.

A. Isometric force response characteristics resulting from muscle stimulation in the rat hindlimb

In order to perform FES control, the responses produced from stimulation of muscles, activated both in isolation and in combination, must be reliable and easily predicted. In the present study, we demonstrated that these requirements were met using the rat hindlimb preparation. The magnitude of evoked force increased systematically up to a plateau level with increasing stimulation strength (see Fig. 2A) while the direction only varied slightly (see Fig. 2B). We found that the relationship between evoked magnitude and stimulation strength was very well described as a sigmoid, as has been described previously for rats, other animals, and humans [19, 26, 35, 36]. Although nonparametric models could in principle be used to characterize recruitment curves with better accuracy, the high goodness of fit found here (see Fig. 4) suggests that any such increases would be minimal.

A significant result of the present experiments is the demonstration that forces evoked by separate muscles combined linearly. The linear combination of evoked forces is commonly assumed in FES applications although it is not usually directly evaluated. There are many factors that might be expected to bring about nonlinear interactions between muscles. The experimental design used here, including the mechanical isolation of the hindlimb and the configuration of electrodes, minimized these potential interactions. In particular, the design of the common return electrode was critical in achieving linear muscle interactions. The large surface area of the common return used in these experiments prevented current spillover to adjacent musculature during intramuscular stimulation. In preliminary experiments in which we used standard return electrode configurations consisting of a single sub-dermic needle [35], we observed substantial nonlinear interactions between muscles. The importance of the return electrode configuration might be particularly important for the rat, since the small size of the rat hindlimb will tend to increase the density of current flowing to the return electrode and therefore increase the amount of potential current spillover. Interestingly, recent work [40] has shown that similar linear combination of muscle forces is observed in human FES systems, suggesting that the properties of force production in the rat shown here are similar to that in humans. Note also that if it is necessary to model cases of non-linear interactions in FES, the rat preparation can also be easily used to model cases of non-linear interactions by altering the return electrode configuration.

B. FES control using many muscles

The success of FES applications is often defined by their ability to emulate the characteristics of motor behaviors produced by healthy individuals. This is a very challenging goal since healthy patients flexibly activate many muscles throughout their limbs and body to regulate a multitude of features (e.g. impedance, position, velocity) relevant to motor behaviors. Therefore, the ability to flexibly stimulate many muscles enables a greater number of motor behaviors using FES. Conversely, being restricted to a small number of muscles for FES control fundamentally limits the types and underlying properties of motor tasks. In this study, we showed that it is possible to achieve a high level of accuracy during FES control of isometric forces while stimulating up to eleven muscles (see Fig. 5 and 6). Such accuracy was consistent across multiple experiments and throughout the workspace of the rat hindlimb (see Fig. 6-8), despite using different stimulation commands for different forces. In fact, we were able to accurately control close synergists and not just antagonists, as shown previously, using intramuscular stimulation. These results would enable a FES controller to confidently distribute commands across many muscles to accomplish a given motor behavior. Similarly, fine coordination of synergists allows complex control strategies to be restored, such as those that might be necessary to avoid fatigue or to compensate for uncertainty in force production.

C. The rat hindlimb as a FES controller test bed

There are both advantages and disadvantages to using the rat hindlimb as a test platform for FES controller development. Using animal models such as the rat avoids the simplifying assumptions inherent in computational models. This allows FES control strategies to be evaluated on actual biological tissue rather than on a computational abstraction,

thereby assisting in the translation of these strategies to human patients. Rats, in particular, are an attractive animal model for FES control development. Alternate animal models such as cats or rabbits are more costly and difficult to maintain. Further, rats are commonly used as models for spinal cord injury, potentially allowing FES control strategies to be tested directly to restore motor function in their paralyzed limbs or to ameliorate the consequences of spinal cord injury

Other laboratories have used rat models to test simple FES controllers for these same reasons [14, 26, 37]. This study builds upon that previous work to demonstrate systematically that, with appropriate experimental procedures, the rat can be used for FES control development. In particular, we describe procedures to maintain mechanical isolation of the rat hindlimb and suitable configurations for stimulation and return electrodes. We also demonstrate that muscles can reliably be activated independently of one another and that simultaneous activation of multiple muscles combines linearly, a basic assumption behind many FES applications. Furthermore, using a larger number of muscles than previous studies enables the evaluation of muscle interactions and how to resolve muscle redundancy. This evaluation of isometric force control, although not directly relevant to motion control, allows us to quantify the limits on accuracy of feedforward FES. This quantification provides important information for investigators attempting to create combined feedforward/feedback systems by specifying the amount of error that feedback control would have to compensate for in order to produce accurate control. These features all establish the rat as a good platform for FES controller development.

In addition to these advantages, there are also potential disadvantages to this preparation when investigating FES controller development. First, the small size of the rat hindlimb required us to develop new methods to isolate the limb mechanically and allow for independent muscle activations. The small size of the limb also likely precludes the ability to perform nerve stimulation for many muscles, as is commonly done in human FES studies. We note, however, that by placing electrodes near to motor points in muscles we were able to evoke substantial forces, even for broad muscles such as biceps femoris posterior (compare Fig. 2 of this paper using intramuscular electrodes with Fig. 2 of Yeo et al. 2011 [24] using nerve stimulation).

Finally, we have only evaluated the use of this preparation for isometric force control, not for motion control. Although many real life tasks require the control of forces, most applications of FES also involve the control of limb movement. It should be possible to develop FES motion controllers for the rat using motion tracking systems and this is a possibility we are currently pursuing. However, it is important to note that FES motion controllers developed for the rat might differ substantially from ones that can be used in humans. Based simply on the difference in limb size between rats and humans, one would expect important differences in the dynamics of their limbs. For instance, recent work has suggested that passive elasticity of muscles should be more important than limb inertia in motor control for the rat, whereas the opposite should be true for motor control in humans [38, 39]. This difference should be kept in mind when using the rat hindlimb to develop FES control strategies that will be applied to humans.

D. Summary

In summary, we have described a rat model that can be used as a test bed for multi-muscle FES controller development. We have validated that we can achieve independent muscle activation in this preparation and that muscle forces combine linearly. In addition to demonstrating accurate open loop FES control of isometric forces distributed throughout the workspace of the limb using many muscles, we evaluated how characteristics of electrical stimulation could be affecting the resulting performance. Even though we focused on open loop FES controllers, we believe our results can also improve feedback FES controllers by enabling such controllers to rely less on feedback. We believe that this study not only serves as a benchmark for the performance of open loop FES control but also raises important considerations for FES controller development. Our research can be readily extended to increase the task difficulty by incorporating additional force components, moments, and motion. Additionally, the model for muscle recruitment can be systematically evaluated using our test platform to uncover ways to further improve open loop FES control. In the end, we believe this work will further the development and validation of advanced FES controllers that can be applied directly to improve the lives of human patients.

REFERENCES

[1] Peckham, P.H. and J.S. Knutson, *Functional electrical stimulation for neuromuscular applications*, in *Annual Review of Biomedical Engineering*. 2005, Annual Reviews: Palo Alto. p. 327-360.

[2] Grill, W.M., et al., *Emerging clinical applications of electrical stimulation: Opportunities for restoration of function.* Journal of Rehabilitation Research and Development, 2001. **38**(6): p. 641-653.

[3] Creasey, G.H., et al., *Clinical applications of electrical stimulation after spinal cord injury.* The journal of spinal cord medicine, 2004. **27**(4): p. 365-75.

[4] Davis, J.A., et al., *Preliminary performance of a surgically implanted neuroprosthesis for standing and transfers - Where do we stand?* Journal of Rehabilitation Research and Development, 2001. **38**(6): p. 609-617.

[5] Harkema, S., et al., *Effect of epidural stimulation of the lumbosacral spinal cord on voluntary movement, standing, and assisted stepping after motor complete paraplegia: a case study.* Lancet, 2011. **377**(9781): p. 1938-1947.

[6] Marsolais, E.B. and R. Kobetic, *Functional electrical stimulation for walking in paraplegia.* Journal of Bone and Joint Surgery-American Volume, 1987. **69A**(5): p. 728-733.

[7] Gallien, P., et al., *Restoration of gait by functional electrical stimulation for spinal-cord injured patients.* Paraplegia, 1995. **33**(11): p. 660-664.

[8] Crago, P.E., R.J. Nakai, and H.J. Chizeck, *Feedbacm regulation of hand grasp opening and contact force during stimulation of paralyzed muscle.* IEEE Transactions on Biomedical Engineering, 1991. **38**(1): p. 17-28.

[9] Grill, J.H. and P.H. Peckham, *Functional neuromuscular stimulation for combined control of elbow extension and hand grasp in C5 and C6 quadriplegics.* IEEE transactions on rehabilitation engineering : a publication of the IEEE Engineering in Medicine and Biology Society, 1998. **6**(2): p. 190-9.

[10] Peckham, P.H., et al., *Efficacy of an implanted neuroprosthesis for restoring hand grasp in tetraplegia: A multicenter study.* Archives of Physical Medicine and Rehabilitation, 2001. **82**(10): p. 1380-1388.

[11] Peckham, P.H., et al., *An advanced neuroprosthesis for restoration of hand and upper arm control using an implantable controller*. Journal of Hand Surgery-American Volume, 2002. **27A**(2): p. 265-276.
[12] Popovic, M.B., et al., *Restitution of reaching and grasping promoted by functional electrical therapy*. Artificial Organs, 2002. **26**(3): p. 271-275.
[13] Taylor, P., J. Esnouf, and J. Hobby, *The functional impact of the Freehand System on tetraplegic hand function. Clinical Results.* Spinal Cord, 2002. **40**(11): p. 560-566.
[14] Kanchiku, T., et al., *Neuromuscular electrical stimulation induced forelimb movement in a rodent model*. Journal of Neuroscience Methods, 2008. **167**(2): p. 317-326.
[15] Zimmermann, J.B., K. Seki, and A. Jackson, *Reanimating the arm and hand with intraspinal microstimulation*. Journal of Neural Engineering, 2011. **8**(5): p. 9.
[16] Miller, L.E., et al., *Restoration of hand use following paralysis: A demonstration of cortically controlled functional electrical stimulation.* Neuroscience Research, 2008. **61**: p. S30-S30.
[17] Pohlmeyer, E.A., et al., *Toward the Restoration of Hand Use to a Paralyzed Monkey: Brain-Controlled Functional Electrical Stimulation of Forearm Muscles.* Plos One, 2009. **4**(6): p. 8.
[18] Fairchild, M.D., et al., *Repetetive hindlimb movement using intermittent adaptive neuromuscular electrical stimulation in an incomplete spinal cord injury rodent model.* Experimental Neurology, 2010. **223**(2): p. 623-633.
[19] Jung, R., et al., *Neuromuscular stimulation therapy after incomplete spinal cord injury promotes recovery of interlimb coordination during locomotion.* Journal of neural engineering, 2009. **6**(5): p. 055010.
[20] Ollivier-Lanvin, K., et al., *Electrical stimulation of the sural cutaneous afferent nerve controls the amplitude and onset of the swing phase of locomotion in the spinal cat.* Journal of Neurophysiology, 2011. **105**(5): p. 2297-2308.
[21] Kutch, J.J. and F.J. Valero-Cuevas, *Muscle redundancy does not imply robustness to muscle dysfunction*. Journal of Biomechanics, 2011. **44**(7): p. 1264-1270.
[22] O'Connor, S.M. and A.D. Kuo, *Direction-Dependent Control of Balance During Walking and Standing.* Journal of Neurophysiology, 2009. **102**(3): p. 1411-1419.
[23] Blana, D., et al., *A musculoskeletal model of the upper extremity for use in the development of neuroprosthetic systems.* Journal of Biomechanics, 2008. **41**(8): p. 1714-1721.
[24] Yeo, S.H., et al., *Estimation of musculoskeletal models from in situ measurements of muscle action in the rat hindlimb*. Journal of Experimental Biology, 2011. **214**(5): p. 735-746.
[25] Ichihara, K., et al., *Neuromuscular electrical stimulation of the hindlimb muscles for movement therapy in a rodent model.* Journal of Neuroscience Methods, 2009. **176**(2): p. 213-224.
[26] Jung, R., et al., *Chronic neuromuscular electrical stimulation of paralyzed hindlimbs in a rodent model.* Journal of Neuroscience Methods, 2009. **183**(2): p. 241-254.
[27] Chizeck, H.J., P.E. Crago, and L.S. Kofman, *Robust closed-loop control of isometric muscle force using pulsewidth modulation*. IEEE Transactions on Biomedical Engineering, 1988. **35**(7): p. 510-517.
[28] Valero-Cuevas, F.J., *A Mathematical Approach to the Mechanical Capabilities of Limbs and Fingers.* Progress in Motor Control: a Multidisciplinary Perspective, 2009. **629**: p. 619-633.
[29] Tresch, M. and E. Bizzi, *Responses to spinal microstimulation in the chronically spinalized rat and their relationship to spinal systems activated by low threshold cutaneous stimulation.* Experimental Brain Research, 1999. **129**(3): p. 401-416.
[30] Huijing, P.A., *Muscular force transmission: A unified, dual or multiple system? A review and some explorative experimental results.* Archives of Physiology and Biochemistry, 1999. **107**(4): p. 292-311.
[31] Maas, H. and T.G. Sandercock, *Are skeletal muscles independent actuators? Force transmission from soleus muscle in the cat.* Journal of Applied Physiology, 2008. **104**(6): p. 1557-1567.
[32] Popovic, D., L. Baker, and G.E. Loeb, *Recruitment and Comfort of BION Implanted Electrical Stimulation: Implications for FES Applications.* IEEE Transactions on Neural Systems and Rehabilitation Engineering, 2007. **15**(4): p. 577-586.
[33] Klimstra, M. and E.P. Zehr, *A sigmoid function is the best fit for the ascending limb of the hoffman reflex recruitment curve.* Experimental brain research, 2008. **186**(1): p. 93-105.
[34] Farahat, W. and H. Herr, *A Method for Identification of Electrically Stimulated Muscle.* 27th Annual International Conference of the Engineering in Medicine and Biology Society, 2005: p. 6225-6228.
[35] Crago, P.E., P.H. Peckham, and G.B. Thrope, *Modulation of muscle force by recruitment during intramuscular stimulation*. IEEE Transactions on Biomedical Engineering, 1980. **27**(12): p. 679-684.
[36] Durfee, W.K. and K.E. Maclean, *Methods for estimating isometric recruitment curves of electrically stimulated muscle*. IEEE Transactions on Biomedical Engineering, 1989. **36**(7): p. 654-667.
[37] Song, W.G. and S.F. Giszter, *Adaptation to a Cortex-Controlled Robot Attached at the Pelvis and Engaged during Locomotion in Rats.* Journal of Neuroscience, 2011. **31**(8): p. 3110-3128.
[38] Hooper, S., et al., *Neural control of unloaded leg posture and of leg swing in stick insect, cockroach, and mouse differs from that in larger animals.* Journal of Neuroscience, 2009. **29**(13): p. 4109-19.
[39] Wu, M., et al., *Passive elastic properties of the rat ankle.* Journal of Biomechanics, 2012. **45**(9): p. 1728-32.
[40] Schearer, E., et al., *Optimal Sampling of Recruitment Curves for Functional Electrical Stimulation Control.* EMBS, 2012.